The EMBO Journal Vol. 21 No. 17 pp. 4539–4549, 2002

Defects in cytokinesis, actin reorganization and the contractile vacuole in cells deficient in RhoGDI

Francisco Rivero[1], Daria Illenberger[2], Baggavalli P.Somesh, Heidrun Dislich, Nicola Adam[2] and Ann-Kathrin Meyer

Institut für Biochemie I, Medizinische Fakultät, University of Cologne, Joseph-Stelzmann-Strasse 52, D-50931 Köln and [2]Department of Pharmacology and Toxicology, University of Ulm, Albert-Einstein-Allee 11, D-89081 Ulm, Germany

[1]Corresponding author
e-mail: francisco.rivero@uni-koeln.de

Rho GDP-dissociation inhibitors (RhoGDIs) modulate the cycling of Rho GTPases between active GTP-bound and inactive GDP-bound states. We identified two RhoGDI homologues in *Dictyostelium*. GDI1 shares 51–58% similarity to RhoGDIs from diverse species. GDI2 is more divergent (40–44% similarity) and lacks the N-terminal regulatory arm characteristic for RhoGDI proteins. Both are cytosolic proteins and do not relocalize upon reorganization of the actin cytoskeleton. Using a two-hybrid approach, we identified Rac1a/1b/1c, RacB, RacC and RacE as interacting partners for GDI1. Cells lacking GDI1 are multinucleate, grow slowly and display a moderate pinocytosis defect, but rates of phagocytosis are unaffected. Mutant cells present prominent actin-rich protrusions, and large vacuoles that are continuous with the contractile vacuole system. The actin polymerization response upon stimulation with cAMP was reduced, but the motile behavior toward the chemoattractant was unaffected. Our results indicate that GDI1 plays a central role in the regulation of signal transduction cascades mediated by Rho GTPases.

Keywords: actin/contractile vacuole/*Dictyostelium*/Rac/RhoGDI

Introduction

Small GTPases of the Rho family of Ras-related proteins are involved in the reorganization of the actin cytoskeleton in a variety of organisms, thus playing a central role in the regulation of a broad diversity of cellular processes (Van Aelst and D'Souza-Schorey, 1997). Small GTPases act as molecular switches, cycling between an active GTP-bound state and an inactive GDP-bound state. Activation enables Rho GTPases to interact with a multitude of effectors that relay upstream signals to cytoskeletal components, eliciting rearrangements of the actin cytoskeleton (Hall, 1998; Ridley, 2001). The GTP-binding/GTPase cycle is in turn modulated by guanine nucleotide exchange factors (GEFs) and GTPase activating proteins (GAPs). GEFs catalyze the conversion to the GTP-bound state, and GAPs accelerate the intrinsic rate of hydrolysis of bound GTP to GDP. GDP-dissociation inhibitors (GDIs) constitute an additional regulatory element. Rho-specific GDIs apparently display three distinct biochemical activities. First, they are able to block the dissociation of GDP from the Rho GTPase, locking the protein in its inactive GDP-bound state and inhibiting activation by GEFs (Fukumoto *et al*., 1990). Secondly, GDIs are capable of binding to the activated, GTP-bound state of Rho proteins, inhibiting their GTPase activity (Hart *et al*., 1992) and preventing interaction with their effectors (Del Pozo *et al*., 2002). Finally, GDIs stimulate the release of Rho GTPases from cellular membranes, significantly contributing to the subcellular localization of particular Rho GTPases (Michaelson *et al*., 2001). For this activity, the Rho GTPase needs to be post-translationally modified by the incorporation of an isoprenyl moiety at its C-terminus (Hori *et al*., 1991). Furthermore, GDIs participate in a number of interactions resulting in the formation of multiprotein complexes. Among the proteins that have been reported to interact with GDIs are a lipid kinase complex (Tolias *et al*., 1998), members of the ezrin/radixin/moesin family (Takahashi *et al*., 1997), components of the NADPH oxidase complex (Abo *et al*., 1991) and the multidomain protein Vav (Groysman *et al*., 2000).

RhoGDIs have been described in a variety of organisms, including *Caenorhabditis elegans*, yeast and plants. In mammals, three isoforms have been characterized, each displaying a specific pattern of tissue distribution and activity toward Rho proteins (for a review, see Olofsson, 1999). RhoGDIα (or RhoGDI) is ubiquitously expressed, whereas RhoGDIβ (or LyGDI) is present in hematopoietic cells. A third isoform, RhoGDIγ, is expressed predominantly in brain, lung, pancreas, intestine and testis, and, contrary to the cytosolic RhoGDIα and β, is associated with the cytoskeleton and membrane compartments. Mice deficient in LyGDI display only subtle alterations of the immunological functions, probably due to compensation by RhoGDI (Yin *et al*., 1997). Deficiency of RhoGDI in mice leads to renal failure and impaired fertility (Togawa *et al*., 1999). However, the effects of RhoGDI deficiency, in particular on cytoskeleton-dependent processes, have not been investigated at the cellular level.

Dictyostelium discoideum is a well-established model organism to investigate the components of the actin cytoskeleton and the elements involved in their complex regulatory pathways (Noegel and Schleicher, 2000). Up to 15 genes coding for Rho-related proteins have been identified in this organism, but most of them are largely uncharacterized (Rivero *et al*., 2001). Rac1a/1b/1c, RacF1/F2 and to a lesser extent RacB and the GTPase domain of RacA (a member of the novel subfamily of RhoBTB proteins) can be grouped in the Rac subfamily. None of the additional *Dictyostelium* Rho-related proteins belong to any of the well-defined subfamilies, like Rac,

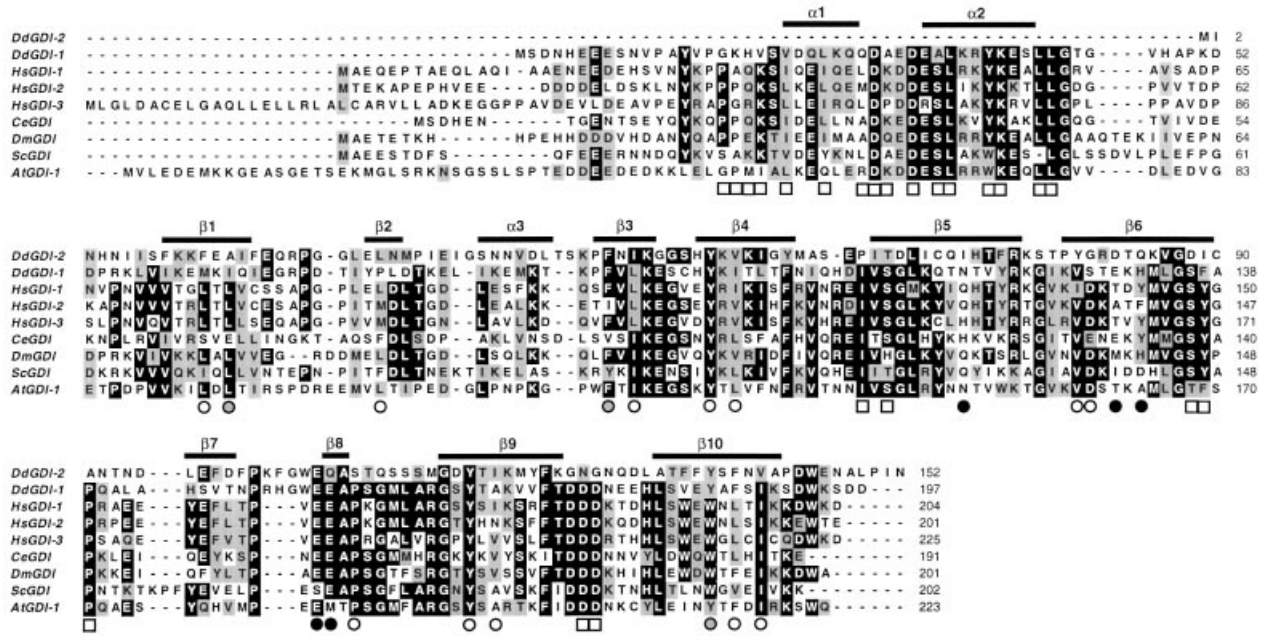

Fig. 1. Multiple alignment of *Dictyostelium* and representative RhoGDI proteins. Sequences were aligned with ClustalX and default parameters, and the output file was subsequently edited manually as described previously (Rivero *et al*., 2001). Dashes indicate gaps introduced for optimal alignment. Residues identical or similar in at least 60% of the sequences are boxed in black or grey, respectively. Secondary structure elements as determined for human LyGDI (Scheffzek *et al*., 2000) are indicated on top of the aligned sequences. Residues involved in the formation of the isoprenyl-binding pocket, as determined for bovine RhoGDI (Hoffman *et al*., 2000), are indicated by open or gray circles under the aligned sequences. Gray circles indicate residues of the 'hydrophobic triad' critical for binding of the distal isoprene unit. Closed circles indicate residues involved in the formation of an acidic patch in the isoprenyl-binding pocket. Important residues involved in interactions with the Rho GTPase, as compiled for bovine RhoGDI and human LyGDI, are indicated by open squares. Accession numbers are: *D.discoideum* RhoGDI1, AY044085; RhoGDI2, AY044086. *Homo sapiens* RhoGDI1 (or α), X69550; RhoGDI2 (or β), L20688; RhoGDI3 (or γ), U82532. *C.elegans*, U36431. *Drosophila melanogaster*, AE003515. *Saccharomyces cerevisiae*, Z74183. *Arabidopsis thaliana* RhoGDI1, AAF70843.

Cdc42 or Rho. To better understand the role of signal transduction cascades involving Rho GTPases in cytoskeleton-dependent processes, we have undertaken the functional characterization of a *Dictyostelium* Rho-GTPase dissociation inhibitor, GDI1. Additionally, we found a second RhoGDI homologue, GDI2, in the *Dictyostelium* genome, which is more divergent and lacks the N-terminal regulatory arm characteristic for GDI proteins. We have studied extensively the impact of the disruption of GDI1 on processes regulated by cytoskeleton rearrangements. Our results indicate that GDI1 plays a critical role in the regulation of signal transduction cascades mediated by a subset of Rho GTPases.

Results

Cloning and sequence analysis of Dictyostelium RhoGDI proteins

We identified two genes encoding RhoGDI proteins in *Dictyostelium*. The *rdiA* gene encodes RhoGDI1 (referred to as GDI1), a protein of 197 amino acids (calculated molecular mass of 22 340). The *rdiB* gene encodes RhoGDI2 (referred to as GDI2), a protein of 152 amino acids (calculated molecular mass of 17 280). Southern blot analyses performed under high and low stringency conditions and extensive analysis of the *Dictyostelium* genomic sequence databases indicated that each gene is present as a single locus (data not shown). Similarity of GDI1 to diverse RhoGDIs ranged between 51% and 58% (33–37% identity) and was evenly distributed along the entire peptide sequence (Figure 1). GDI2 aligned to the β-strand-rich C-terminal domain of RhoGDIs, with which it showed only 40–45% similarity (20–25% identity). This domain has an immunoglobulin-like fold that contains a hydrophobic pocket for insertion of the isoprenyl moiety of the Rho GTPase (Hoffman *et al*., 2000). The non-polar residues that form this pocket are conserved both in GDI1 and GDI2 (Figure 1, open and gray circles), particularly the 'hydrophobic triad' constituted by L77, F102 and W194 of bovine RhoGDI (Figure 1, gray circles). The pattern of expression of the *rdiA* and *rdiB* genes during development and the dynamics of subcellular distribution of both GDIs fused to green fluorescent protein (GFP) are shown in Supplementary figures 1 and 2 (Supplementary data are available at *The EMBO Journal* Online).

Interaction of GDI1 and GDI2 with Rho GTPases

To identify potential binding partners for GDI1 and GDI2, we performed a two-hybrid analysis, using diverse GTPases as bait and GDIs as prey. All constructs we attempted for RacH displayed autoactivation of the β-galactosidase activity used as a reporter. RacH was therefore excluded from the analysis. GDI1 interacted with Rac1a/1b/1c, RacB, RacC and RacE, as well as with three human Rho GTPases, Rac1, Cdc42 and RhoA. There was no interaction with RasG, which has a prenylation motif, indicating that GDI1 specifically binds to GTPases of the Rho family. Positive interactions in the two-hybrid analysis were confirmed in translocation experiments.

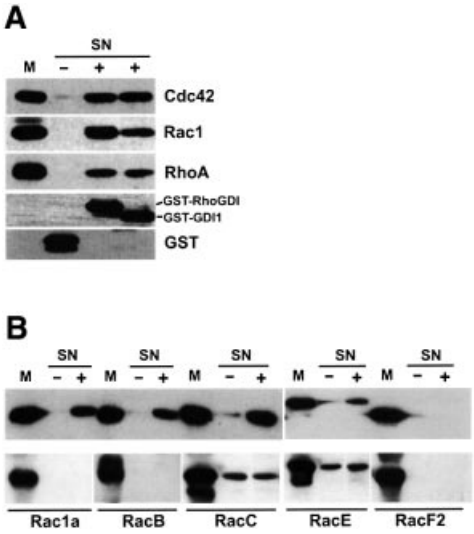

Fig. 2. Interaction of RhoGDI proteins with Rho GTPases. (**A**) Translocation of human Rho GTPases by *Dictyostelium* GDI1. Membrane fractions of insect cells infected with baculovirus encoding human Cdc42, Rac1 or RhoA were incubated with 40 μM purified bacterially expressed GST (lane marked with –), GST–RhoGDI or GST–GDI1 (lanes marked with +). The membranes were sedimented by centrifugation and aliquots of the supernatants were subjected to SDS–PAGE. The aliquots of membrane fraction (M) correspond to the percentage of the analyzed supernatants (SN). Immunoblotting was performed using antibodies reactive against Cdc42, Rac1, RhoA, or GST as indicated. (**B**) Translocation of *Dictyostelium* Rho GTPases by GDI1 (upper panel) and GDI2 (lower panel). Membrane fractions of insect cells infected with baculovirus encoding the indicated *Dictyostelium* GST-tagged Rho GTPases were incubated in the absence (–) or presence (+) of 40 μM purified bacterially expressed His-tagged GDI1 or GDI2. Samples were processed as in (A) and GTPases were detected with an antibody reactive against GST. Labeling of lanes is essentially as in (A). In these experiments, His-tagged GDI1 and GDI2 were always recovered in the supernatant.

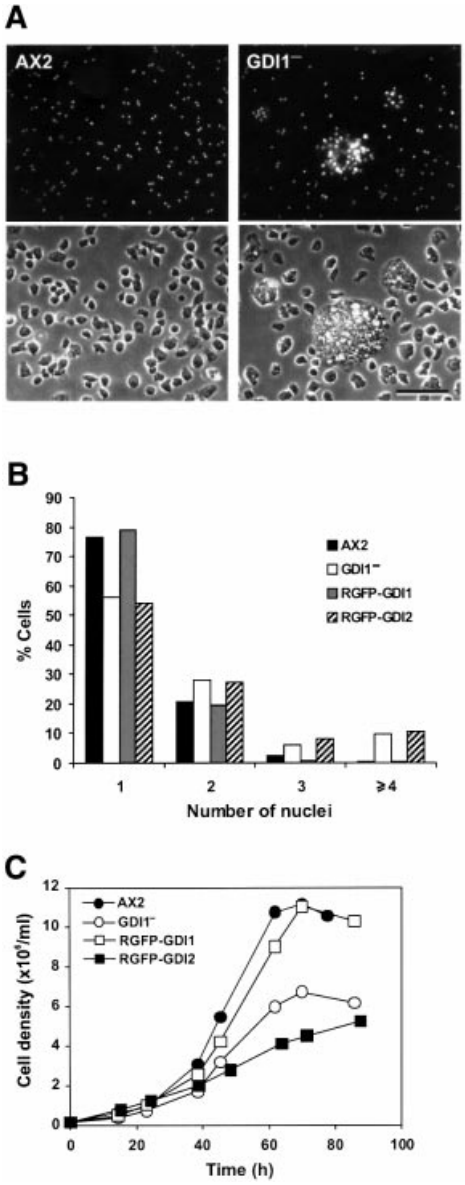

Fig. 3. GDI1⁻ cells display cytokinesis and growth defects. (**A**) DAPI staining (top panels) and corresponding phase contrast (bottom panels) images of wild-type and mutant cells grown on glass coverslips. Scale bar, 50 μm. (**B**) Distribution of the number of nuclei in GDI1⁻ and complementation mutants grown on coverslips. In the GDI1⁻ mutant, cells with four or more nuclei account for ~10% of the population. (**C**) Growth of GDI1 null and complementation mutants in shaking suspension. The growth and cytokinesis defects of GDI1⁻ were restored after re-expression of GDI1. Curves are representative of at least three independent determinations, each performed in duplicate.

We analyzed solubilization of recombinant isoprenylated Rho GTPases from membranes of baculovirus-infected insect cells by bacterially expressed, purified GDI1. Glutathione *S*-transferase (GST)–GDI1 was capable of extracting human Cdc42, Rac1 and RhoA to an extent similar to or slightly lower than bovine GST–RhoGDI (Figure 2A). His-tagged GDI1 was capable of extracting GST-tagged *Dictyostelium* Rac1a, RacB, RacC and RacE. Interaction with RacE was comparatively weak. It was surprising that no interaction with RacF1 and RacF2 was detected in the two-hybrid analysis, in spite of the fact that both are more closely related to Rac1a/1b/1c than RacB, RacC or RacE. However, the translocation experiment confirmed this result (Figure 2B, upper panel).

In two-hybrid experiments, GDI2 did not interact with any of the *Dictyostelium* or human Rho GTPases assayed. This result was verified in translocation experiments with His-tagged GDI2 (Figure 2B, lower panel). This could be explained by the absence of an N-terminal regulatory domain that harbors most of the residues involved in the interaction with the Rho GTPase (Figure 1). To further test the ability of GDI2 to interact with Rho proteins, we made a chimeric construct consisting of the N-terminal domain of GDI1 fused to GDI2. However, this construct failed to display interaction with any of the Rho GTPases tested in the two-hybrid assay or in translocation experiments (data not shown), pointing at the core domain of GDI2 as responsible for lack of interaction.

Generation and characterization of a GDI1⁻ mutant

To gain insight into the function of GDI1 *in vivo*, we have generated a knockout cell line by homologous recombination (see Supplementary figure 3). During microscopic inspection of mutant cells growing on a substrate, we observed very large cells scattered all over the culture dishes. These cells were massively multinucleated, as revealed by staining with the nuclear marker

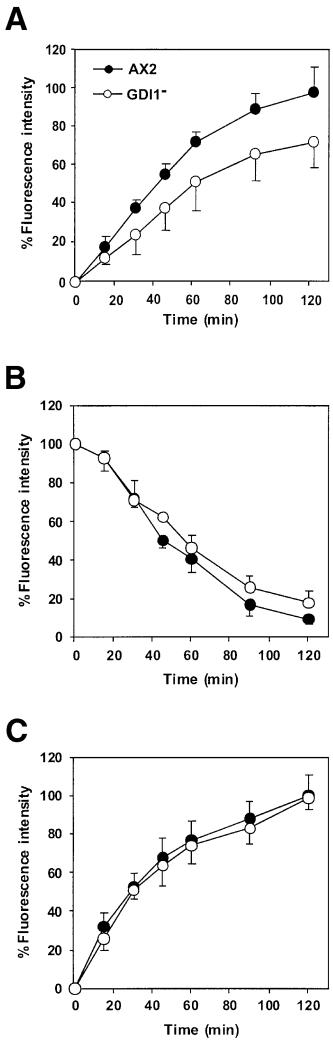

Fig. 4. Endocytosis of wild-type and GDI1⁻ cells. (**A**) Pinocytosis of FITC-dextran. Cells were resuspended in fresh axenic medium at 5×10^6 cells/ml in the presence of 2 mg/ml FITC-dextran. Fluorescence from the internalized marker was measured at selected time points. (**B**) Fluid-phase exocytosis of FITC-dextran. Cells were pulsed with FITC-dextran (2 mg/ml) for 3 h, washed and resuspended in fresh axenic medium. Fluorescence from the marker remaining in the cell was measured. (**C**) Phagocytosis of TRITC-labeled yeast cells. *Dictyostelium* cells were resuspended at 2×10^6 cells/ml in fresh axenic medium and challenged with a 5-fold excess fluorescent yeast cells. Fluorescence from internalized yeasts was measured at the designated time points. Data are presented as relative fluorescence, AX2 being considered 100%, and all values are the average ± standard deviation of at least three independent experiments.

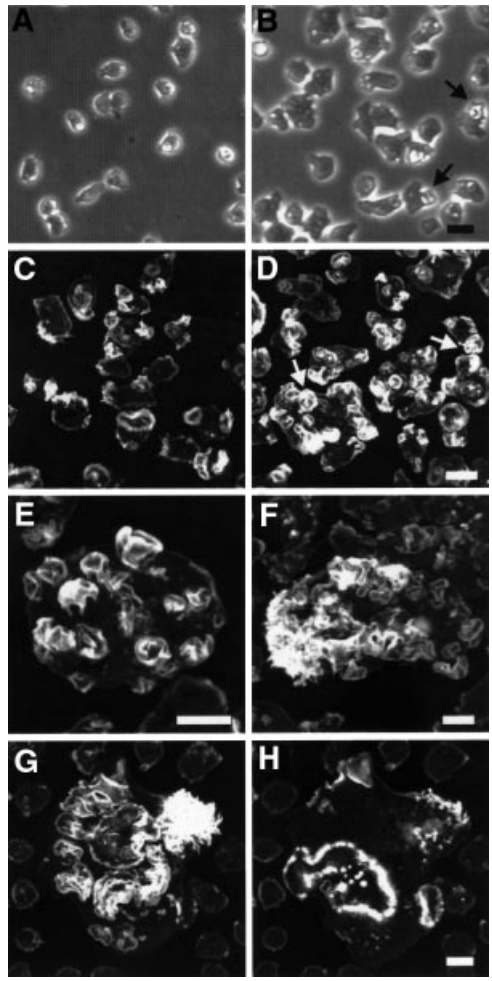

Fig. 5. Morphology and F-actin distribution in GDI1⁻ cells. (**A**) AX2 and (**B**) GDI1⁻ vegetative cells growing on petri dishes in axenic medium. Phase–contrast images. GDI1⁻ cells are larger and present very prominent crown-like structures (arrows). (**C**) AX2 and (**D**) GDI1⁻ cells grown overnight on coverslips in axenic medium were fixed with picric acid/paraformaldehyde and stained with TRITC-phalloidin. Arrows indicate examples of large actin-rich crown-like structures. Pictures are the maximum projection of 17–30 confocal sections 405 nm apart. (**E**) Closer view of a large GDI1⁻ cell displaying actin enrichment at numerous crown-like structures. Maximum projection of 23 confocal sections 405 nm apart, excluding the contact surface. (**F** and **G**) F-actin distribution in GDI1⁻ giant cells. Maximum projection of 34 or 30 confocal sections, respectively, 365 nm apart excluding the contact surface. Note the prominent crown-like and lamellar structures, and the accumulation of microspikes at one end of the cell. (**H**) Maximum projection of 10 confocal sections 365 nm apart from the bottom of the same cell as in (G) showing F-actin accumulation at regions of contact with the substrate. Scale bars represent 10 μm. Except for (E) and (F) the bar on the right picture applies also to the picture on the left.

4′,6-diamidino-2-phenylindole (DAPI), with as many as 40 nuclei in some cases (Figure 3A). Approximately 10% of the mutant cells had four or more nuclei, compared with 0.6% in AX2 (Figure 3B). The same extent of multi-nuclearity was also observed in cells growing in suspension. On average, GDI1⁻ cells were moderately, but significantly ($P < 0.001$; Student's *t*-test), larger (12.70 ± 3.10 μm; $n = 340$) than AX2 cells (11.68 ± 1.99 μm; $n = 334$). The cytokinesis defect could account for this alteration of the cell size.

Under standard laboratory conditions, mutant cells grew with a slightly prolonged doubling time during log phase (12.0 h) when compared with AX2 (10.8 h), and reached saturation at a lower cell density (6.8×10^6 cells/ml) than the wild-type strain (11.1×10^6 cells/ml; Figure 3C). An impaired growth rate was expected due to the cytokinesis defect described above. To investigate the possible additional contribution of an alteration of the rate of pinocytosis, we quantitated this process and found that the rate of internalization of the fluid phase marker FITC-dextran by GDI1⁻ cells was 74% of that of AX2 cells ($P < 0.001$; Student's *t*-test; Figure 4A). However, GDI1⁻ cells were able to release the fluid phase marker at a rate not significantly different from that of AX2 cells (Figure 4B). Finally, phagocytosis of TRITC-labeled yeast

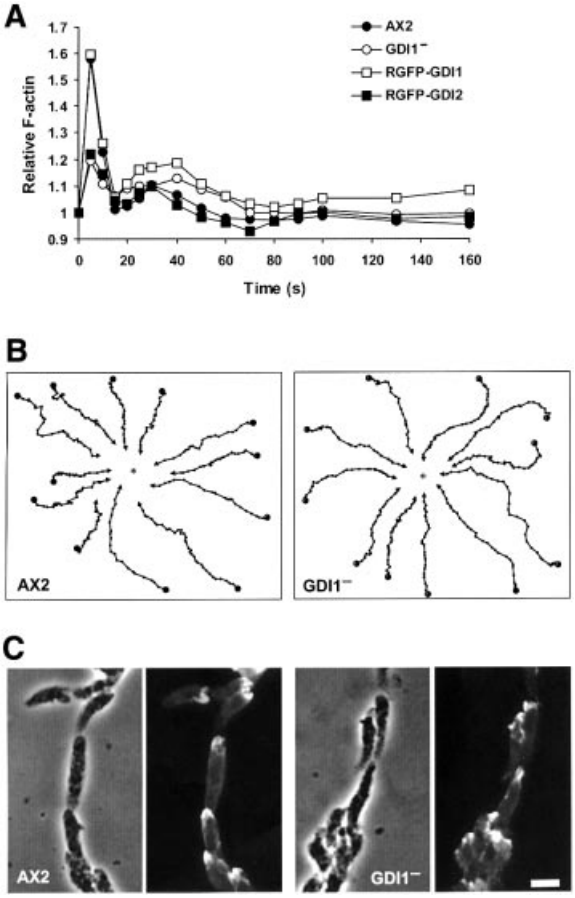

Fig. 6. Actin polymerization and chemotactic response upon cAMP stimulation of aggregation competent cells. (**A**) F-actin polymerization responses of GDI1⁻ and complementation mutants. The relative F-actin content was determined by TRITC-phalloidin staining of cells fixed at the indicated time points after stimulation with 1 μM cAMP. Each data point represents the average of at least three independent measurements. For the sake of clarity, error bars are not shown. Standard deviations fell between 4% and 11% of the average values. In GDI1⁻ cells, the initial response of actin polymerization and depolymerization was reduced, and was restored after re-expression of GDI1. (**B**) Chemotactic movement toward a micropipette filled with 0.1 mM cAMP. Cells were starved for 6 h, allowed to sit on a glass coverslip and stimulated with a micropipette filled with 0.1 mM cAMP. Images of chemotaxing cells were captured every 30 s for up to 60 min. DIAS software was used to analyze cell movement and generate the migration paths. The asterisks indicate the position of the micropipette tip. GDI1⁻ cells display an apparently normal chemotactic response. (**C**) Morphology of aggregation competent wild-type and GDI1⁻ cells. Cells were prepared as in (B), fixed and stained with mAb Act-1 to visualize actin. GDI1⁻ cells are well polarized and build cell streams. Scale bar, 10 μm.

cells occurred at the same rate in AX2 and GDI1⁻ cells (Figure 4C). Growth rates on nutrient agar plates with bacteria as a food source were also similar for both strains (data not shown), indicating further that phagocytosis is not significantly impaired in the GDI1⁻ cells.

Changes in actin distribution in GDI1⁻ cells

Microscopic inspection of cells growing in axenic medium in Petri dishes revealed the presence of conspicuous crown-like structures on the dorsal and lateral surfaces of GDI1⁻ cells (Figure 5A and B). To correlate this observation with changes in the actin distribution, we generated maximum projection images from confocal sections

Table I. Analysis of cell motility of GDI1⁻ mutant

	AX2	GDI1⁻
Speed (μm/min)	11.81 ± 3.15	11.04 ± 4.57
Persistence (μm/min × deg)	4.06 ± 1.87	4.09 ± 2.23
Directionality	0.80 ± 0.11	0.73 ± 0.23

Time-lapse image series were captured and stored on a computer hard drive at 30 s intervals. The DIAS software was used to trace individual cells along image series and calculate motility parameters. Persistence is an estimation of movement in the direction of the path. Directionality is calculated as the net path length divided by the total path length, and gives 1.0 for a straight path. Values are mean ± standard deviation of 76 (AX2) or 176 (GDI1⁻) cells from at least three independent experiments. Both strains did not differ statistically in their motility behavior (Student's *t*-test).

through fixed cells stained with TRITC-phalloidin, a procedure that renders images with a pseudo-three dimensional appearance. AX2 cells display a smooth cortical actin staining, with enrichment at filopods and membrane protrusions (Figure 5C). Besides this smooth cortical staining, intensely labeled structures were apparent in GDI1⁻ cells. They had most frequently a flower-like appearance, sometimes a knob-like shape (Figure 5D). These protrusions could be observed throughout the whole cell population, and in many cases, they covered the dorsal and lateral surfaces of the cell (Figure 5E). Giant GDI1⁻ cells displayed a wide range of patterns of actin distribution. In many cases, they were rich in prominent lamellar actin-rich structures and were frequently accompanied by the accumulation of microspikes at one end of the cell (Figure 5F and G). They also displayed very intensely stained rims and dots at regions where the cell contacts the substrate (Figure 5H).

Treatment of GDI1⁻ cells with the actin-depolymerizing agent cytochalasin A resulted in cell rounding and accumulation of actin at the cell periphery, indicating that the protrusions characteristic of these cells are actin driven (data not shown).

Actin polymerization and chemotaxis of GDI1⁻ cells

Aggregation competent cells move actively toward a cAMP gradient. Upon cAMP stimulation, fast and highly transient changes in the F-actin content take place that correlate with changes in cell behavior (Hall *et al*., 1988). Five seconds after stimulation of AX2 cells with cAMP, a 1.6-fold increase in the amount of F-actin was observed that decreased rapidly to basal levels after 20 s. A second, much lower peak followed immediately and lasted until ~50 s. GDI1⁻ cells showed a lower increase in the first F-actin peak (1.2-fold), whereas the second peak was not altered (Figure 6A). Basal F-actin levels were found to be already decreased in the GDI⁻ mutant relative to AX2, both in vegetative (68.0 ± 7.5%) and in aggregation competent (82.7 ± 7.3%) cells.

In a micropipette-based assay, AX2 and GDI⁻ cells behaved similarly upon stimulation with 0.1 mM cAMP; cells became polarized, accumulated actin at the leading front, formed streams and migrated toward the tip of the micropipette (Figure 6B and C). GDI⁻ cells did not differ significantly from the wild type in motility parameters like speed, persistence and directionality (Table I). Therefore,

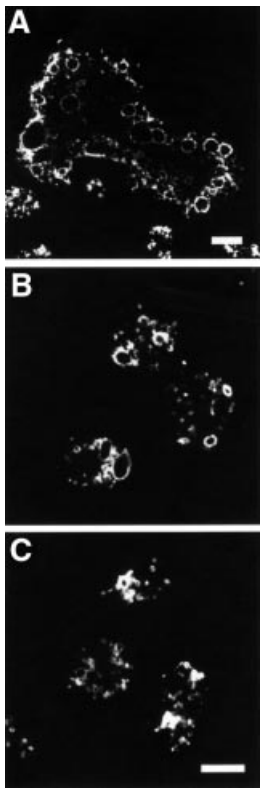

Fig. 7. GDI1 is involved in the regulation of the contractile vacuole. Confocal immunofluorescence images of cells grown overnight on coverslips in axenic medium, fixed with picric acid/paraformaldehyde and immunostained with mAb 221-35-2 (a marker of membranes of the contractile vacuole and the endo/lysosomal system). (**A**) Staining around the numerous large vacuoles of a GDI$^-$ giant cell. Normal-sized mutant cells (**B**) display larger vacuoles as compared with the wild-type strain (**C**). Scale bars are 10 μm.

the impairment in actin polymerization of GDI1$^-$ cells in response to cAMP is not of such an extent as to preclude an apparently normal chemotactic response. In fact, under all conditions studied, the timing and morphology of the developmental process appeared essentially unaltered in the mutant strain (data not shown).

GDI1$^-$ cells have a defect in the contractile vacuole system

Microscopic inspection of mutant cells growing on a substrate brought to our attention the presence of abundant vacuoles of large size in giant GDI1$^-$ cells that conferred them a foamy appearance (Figure 3A). Immunofluorescence studies revealed no staining of this membrane compartment either for protein disulfide isomerase, an endoplasmic reticulum protein (Monnat *et al*., 1997), or for vacuolin, a marker for vacuoles of a post-lysosomal compartment (Rauchenberger *et al*., 1997). Immunostaining for the A subunit of the V/H$^+$-ATPase, a protein present on membranes of the contractile vacuole and the endo/lysosomal system of *Dictyostelium* (Jenne *et al*., 1998), clearly demonstrated that large vacuoles are continuous with the contractile vacuole system, a tubular–vesicular network found preferentially in the cell periphery (Figure 7A) that is involved in osmoregulation and calcium homeostasis (Clarke and Heuser, 1997). Normal-sized mutant cells also displayed larger vacuoles as compared with the wild-type strain (Figure 7B and C). To analyze the functional integrity of the contractile vacuole system, we examined the osmo-sensitivity of GDI1$^-$ cells. Viability and behavior of the contractile vacuole system were unaltered in GDI1$^-$ cells both under hypo-osmotic (2 h in water) and hyper-osmotic (2 h in 0.4 M sorbitol) conditions (data not shown).

Partial recapitulation of the GDI1$^-$ phenotype by expression of constitutively active Rho GTPases

Expression in GDI1$^-$ cells of a GFP fusion of GDI1 (RGFP–GDI1 strain), but not of GDI2 (RGFP–GDI2 strain), a protein presumed to be present only at late stages of development, reverted the cytokinesis, growth and actin polymerization defects, confirming that the phenotype observed in GDI1$^-$ cells specifically arises from the absence of GDI1 (Figures 3B, 3C and 6A).

RhoGDIs can be thought of as negative regulators of some Rho GTPases by maintaining them as inactive cytosolic forms that are unable to interact with their regulators and downstream effectors. To test this hypothesis and to investigate whether a particular phenotype of GDI1$^-$ cells can be linked to a particular GDI1-interacting Rho GTPase, we expressed constitutively active forms of GFP-tagged RacC and RacE in *Dictyostelium* cells. Mutants expressing constitutively active Rac1 isoforms have been extensively studied (Chung *et al*., 2000; Dumontier *et al*., 2000; Palmieri *et al*., 2000) and mutants expressing constitutively active RacB are being investigated elsewhere (D.Knecht, personal communication). Both RacC-L64 and RacE-V20 mutants behaved similarly. Suspension cultures reached saturation at low cell densities (~5 × 10^6 cells/ml; Figure 8A). This growth defect can be explained, at least in part, by a cytokinesis defect; there was a marked decrease in the proportion of mononucleated cells in favor of multi-nucleated cells (mostly three or four nuclei, in few cases up to 15 nuclei; Figure 8B and C). This defect became less apparent when cells were allowed to grow overnight on a substrate prior to fixation. Very large cells and unusual actin-rich structures were not apparent in any of the strains (Figure 8B), but both mutants displayed a reduced F-actin polymerization response to cAMP with a lower increase in the first F-actin peak and the absence of the second peak (Figure 8D). Our results with RacE-V20 mutant contrast with a previous report by Larochelle *et al*. (1997), who described normal growth and cytokinesis in cells overexpressing the same mutated form of RacE. We attribute these differences to the genetic background of the strains used or to different overexpression levels.

Discussion

We have identified two RhoGDI proteins in *Dictyostelium*, GDI1 and GDI2, and have determined the repertoire of Rho proteins capable of interacting with GDI1: Rac1a/b/c, RacB, RacC and RacE. Absence of interaction with RacA and RacD can be easily attributed to the lack of an isoprenyl moiety. It is well established that this modification is required for the GTPase to interact with the GDI (Hori *et al*., 1991). Structural studies have allowed the determining of which residues of the Rho GTPase are

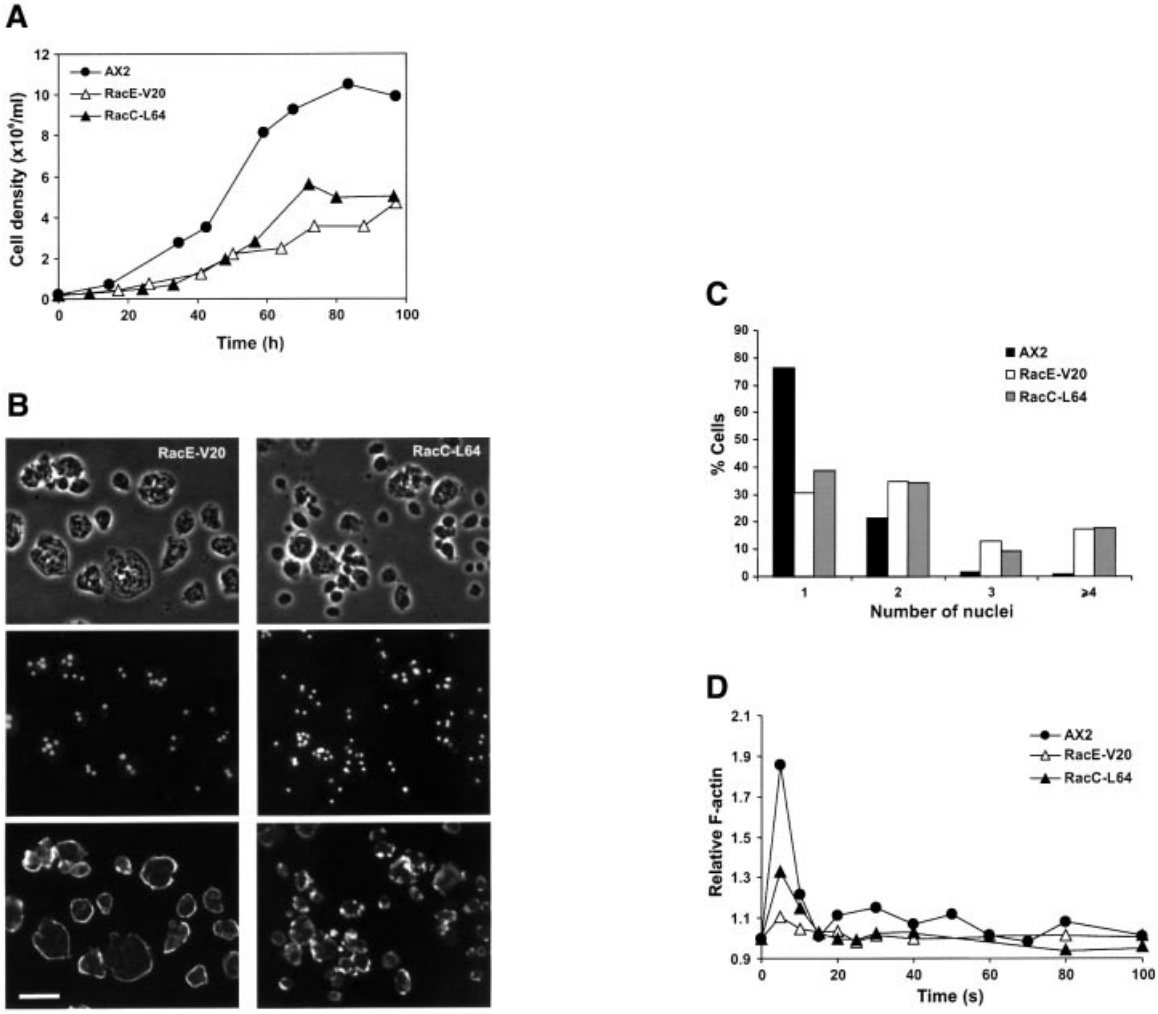

Fig. 8. Expression of constitutively active Rho GTPases RacC-L64 and RacE-V20 fused to GFP partially phenocopy the defects of GDI$^-$ cells. (**A**) Growth in shaking suspension. Curves are representative of two independent determinations, each performed in duplicate. (**B**) Nuclear staining and actin distribution. From top to bottom, phase–contrast, DAPI staining and immunostaining of actin of cells grown in suspension. Cells were allowed to sit for 20 min on coverslips prior to fixation. Scale bar, 25 μm. (**C**) Distribution of the number of nuclei in mutants grown in suspension. (**D**) Actin polymerization upon cAMP stimulation of aggregation competent cells. Experiments were performed as described in Figure 6A. Both mutants display growth, cytokinesis and actin polymerization defects.

involved in interactions with the GDI (Hoffman *et al*., 2000; Scheffzek *et al*., 2000). These are (numbering corresponds to human Rac1) Thr35, Tyr64, Arg66 and His103. Thr35 (or serine, as in RacI) is involved in the coordination of the Mg^{2+} ion, and is conserved in all GTPases. Whereas all three other residues are present in Rac1a/b/c, RacB, RacC (Arg66 substituted by Lys) and RacE, substitutions in one or more of these residues might explain lack of interaction of GDI1 with RacG, RacI and RacL, and suggest that RacH, which could not be tested in the two-hybrid analysis, presumably will also not interact. Lack of interaction with RacJ is easy to explain in view of the extensive divergence of the switch regions of this GTPase. More difficult to explain is why no interaction was observed with RacF1/F2, where the residues involved in interaction with GDI are perfectly conserved. It appears that a subtle substitution or post-translational modification elsewhere is responsible for the behavior of RacF1/F2. C-terminal palmitoylation, for example, is in part responsible for the lack of interaction of RhoB and TC10 with RhoGDI (Michaelson *et al*., 2001). However, in RacF1/F2, the most C-terminal cysteine residue, other than the prenylation signal, is part of the A5 helix and is probably not suitable for lipid modification. The only two Rac proteins of *Dictyostelium* that could be palmitoylated at their C-terminus are RacG and RacI, but in these cases, additional amino acid substitutions, as already mentioned, account for the lack of interaction with GDI1.

The presence of a GDI-related protein in *Dictyostelium*, GDI2, is puzzling. Interestingly, ICAP-1, initially described as a protein interacting with the cytoplasmic domain of integrin, binds Rac1 and Cdc42 and displays GDI activity on Cdc42 at least, in spite of a lower degree of similarity than GDI2 with the C-terminal region of RhoGDI (Degani *et al*., 2002). Although sequence analysis indicates that GDI2 could adopt a structure capable of harboring an isoprenyl modification, we could not detect interaction of GDI2 with any of the Rho GTPases tested. This cannot be attributed solely to lack of an N-terminal regulatory arm, as demonstrated in experiments with a

chimeric protein of GDI2 and the N-terminus of GDI1. A single amino acid change from Ile177 in human RhoGDI to an Asn residue at the corresponding position in LyGDI has been reported to account for the 20-fold lower affinity observed for the binding of Cdc42 to LyGDI (Platko *et al*., 1995). An analogous situation can be invoked to explain the behavior of GDI2. It cannot be excluded that isoprenylated GTPases other than Rho proteins, or even isoprenylated proteins not related to GTPases, could interact with GDI2. In support of this, it has been described that RhoGDI is capable of binding to isolated isoprenyl units, although with lower affinity than to the isoprenylated Rho GTPase (Mondal *et al*., 2000).

Rac-dependent signaling pathways regulated by GDI1

The changes in the morphology and the pattern of actin distribution of GDI1$^-$ cells are in accordance with the pivotal role of Rho GTPases in the regulation of different components of the cytoskeleton (Ridley, 2001). The lamellar structures and microspikes apparent on giant GDI1$^-$ cells are similar to those observed in mammalian cells microinjected with dominant active Rac1 and Cdc42, respectively, and more importantly, these changes were reduced by microinjection of RhoGDI (Kozma *et al*., 1995). Remarkably, in a HeLa-derived human cell line induction of the expression of Cdc42-V12 led to the formation of giant multi-nucleated cells and the accumulation of actin in cortical microspikes and in dot-like structures located at the ventral face of the cell (Dutartre *et al*., 1996). This is consistent with the current view of RhoGDI as a negative regulator of Rho-controlled signaling pathways. However, the prominent actin-rich structures characteristic of GDI1$^-$ cells cannot be observed in *Dictyostelium* cells overexpressing constitutively active forms of any of the Rho GTPases able to interact with GDI1; cells overexpressing activated Rac1 isoforms display actin-enriched crown-shaped extensions, although not so prominent as in the GDI1$^-$ mutants (Dumontier *et al*., 2000). Cells overexpressing RacB-V12 form actin-driven spherical protrusions (D.Knecht, personal communication), whereas no noticeable alterations were seen in cells overexpressing RacE-V20 or RacC-L64. Similarly, the cytokinesis defects elicited by overexpression of the same constitutively active GTPases differ from the defect observed in GDI1$^-$ cells; overexpressing mutants do not become massively multi-nucleated and, at least for Rac1, RacC and RacE, the defect is apparent only when cells grow in suspension (Dumontier *et al*., 2000; Palmieri *et al*., 2000).

Rho GTPases also participate in the regulation of endocytic traffic. Activated Rho and Rac stimulate pinocytosis in *Xenopus* oocytes and mammalian cells, respectively (Ellis and Mellor, 2000), and recruitment of activated Rac1 to the plasma membrane induces uptake of latex particles by a mammalian cell line (Castellano *et al*., 2000). By contrast, the same activated GTPases inhibit receptor-mediated endocytosis and, more important, inclusion of RhoGDI prevents this inhibitory effect (Lamaze *et al*., 1996). In *Dictyostelium*, overexpression of constitutively active (but not dominant negative) Rac1 isoforms results in reduced pinocytosis and phagocytosis rates (Dumontier *et al*., 2000; Palmieri *et al*., 2000), whereas overexpression of both constitutively active or dominant-negative RacB is accompanied by reduction of both processes (D.Knecht, personal communication), and RacC stimulates phagocytosis, but reduces pinocytosis (Seastone *et al*., 1998). Although GDI interacts strongly with Rac1, RacB and RacC, phagocytosis is unaffected and pinocytosis is only moderately reduced in GDI1$^-$ cells, indicating that GDI-regulated cycling of the Rho GTPase between cytosol and the plasma membrane is dispensable for a proper functioning of these processes. In addition, signaling pathways controlled by other Rho proteins not regulated by GDI1, like RacG (our unpublished data), as well as other GTPases, like Ras and Ras-related proteins, may be sufficient to ensure functioning of endocytosis.

GDI1$^-$ cells showed low F-actin levels and a lower increase in F-actin polymerization, but a normal chemotactic response to cAMP. By contrast, overexpression of activated Rac1 or RacB resulted in an increased amount of F-actin and, in the case of Rac1, in impaired chemotactic response (Chung *et al*., 2000; D.Knecht, personal communication). Thus, GDI1 seems to act as a global regulator of the actin polymerization process through interaction with Rho GTPases, but is not required for the spatial or temporal regulation of the chemotactic response. Again, activation of Rho proteins not regulated by GDI1, like RacG (our unpublished data), might warrant the establishment of cell polarity in response to the chemoattractant in the absence of GDI1.

Rac signaling and the contractile vacuole function

It is noteworthy that mice lacking RhoGDI present intense vacuolization in the basal side of epithelial cells of the proximal renal tubules and in the seminiferous epithelium, resulting in vacuolar degeneration of these epithelia (Togawa *et al*., 1999). This suggests that RhoGDI might be regulating a compartment functionally equivalent to the contractile vacuole of protists. In support of this, a *Dictyostelium* protein involved in discharge of the contractile vacuole, drainin, is also present in *C.elegans* and humans (Becker *et al*., 1999). The contractile vacuole system is primarily regulated by small GTPases of the Rab family. Expression of dominant-negative forms of RabD or Rab11 results in morphological and functional alterations of the contractile vacuole system (Bush *et al*., 1996; Harris *et al*., 2001). Similar to what has been described in yeast, where both Rho and Rab GTPases are required for vacuole fusion (Eitzen *et al*., 2001), in *Dictyostelium*, both signaling pathways may also be interconnected. The GAP domain of DRG (RacGAP-1), which acts on Rac and Rab pathways, appears to be important for the regulation of the contractile vacuole system (Knetsch *et al*., 2001). It is conceivable that the absence of GDI1 could disturb the equilibrium between the Rac- and Rab-dependent pathways.

The signaling pathways that converge in controlling actin assembly and disassembly and have an impact in diverse cellular processes are intricate and very poorly understood. The fact that the phenotypic alterations displayed by GDI1$^-$ cells can be reproduced only partially by overexpression of the activated form of a particular GDI1-interacting Rho protein is consistent with a role of GDI1 as a global regulator of Rho-dependent signaling pathways by maintaining the equilibrium between GDI-regulated and non-GDI-regulated signaling pathways.

Materials and methods

Sequence analysis

The amino acid sequence of human GDI1 was used as query for TBLASTN searches of the *Dictyostelium* EST database (http://www.csm.biol.tsukuba.ac.jp/cDNAproject.html). This allowed the identification of several cDNA clones for GDI1 and GDI2. In a second step, cDNA sequences were used for BLASTN searches of the *Dictyostelium* genome project database (http://www.uni-koeln.de/dictyostelium/). Genomic clones JC2b55b07 and JAX4b29h11 (for GDI1) and JC2d59b01 (for GDI2) were retrieved from the *Dictyostelium* genome sequencing project and fully sequenced. Sequence analysis was performed with the Wisconsin Package Version 9.0 of the Genetics Computer Group (Madison, WI). *Dictyostelium* GDIs have received following DDBJ/EMBL/GenBank accession Nos: RhoGDI1, AY044085; RhoGDI2, AY044086.

Protein expression and generation of monoclonal antibodies

For expression of recombinant proteins pGEX-2T (Amersham-Pharmacia Biotech, Freiburg, Germany) and pQE30 (Qiagen GmbH, Hilden, Germany) vectors were used. Recombinant GST-fusion and His-tagged proteins were purified from the soluble fraction of bacterial extracts on glutathione–agarose (Amersham-Pharmacia) and Ni^{2+}-NTA agarose (Qiagen), respectively. For mAb production, BALB/c mice were immunized with recombinant GDI1 as described (Jenne *et al*., 1998). Spleen cells were fused with PAIB3AG8I myeloma cells 2 days after the last boost. Hybridomas were screened for their ability to recognize the antigen on ELISA plates and western blots. MAb K8-322–2 recognized GDI1.

Strains, growth conditions and development of D.discoideum

Wild-type strain AX2–214, a derivative of NC-4, is the parent strain of all mutants used in this study. To express GFP fusions of *Dictyostelium* GDIs or Rho GTPases, cDNA fragments were cloned in a frame at its 5′end to the coding region of the red shifted S65T mutant of *Aequoria victoria* GFP in the transformation vector pDEX-GFP (Westphal *et al*., 1997). RacC-Q64L was a kind gift from Dr Menno Knetsch. RacE–G20V was generated from the wild-type cDNA by a PCR-based site directed mutagenesis procedure. Vectors were introduced into AX2 or GDI1$^-$ cells by electroporation. After selection for growth in the presence of G418 (Sigma), GFP-expressing transformants were confirmed by visual inspection under a fluorescence microscope. Disruption of the *rdiA* gene is described in Supplementary figure 3. All strains were grown either in liquid nutrient medium at 21°C with shaking at 160 r.p.m. or on nutrient agar plates with *Klebsiella aerogenes*. For development, cells were grown to a density of 2–3 $\times$ 10^6 cells/ml, washed in 17 mM Soerensen phosphate buffer pH 6.0, and 0.5 $\times$ 10^8 cells were deposited on nitrocellulose filters (Millipore type HA, Millipore, Molsheim, France) and allowed to develop at 21°C as described previously (Rivero *et al*., 1999). Morphology was also studied by allowing 0.5 $\times$ 10^8 cells to develop on 1.2% (w/v) water agar or phosphate-buffered agar plates at 21°C.

Western, Southern and northern blotting

SDS–PAGE and western blotting were performed as described previously (Sambrook and Russell, 2001) using an enhanced chemiluminescence detection system (Amersham-Pharmacia). GST was detected with a polyclonal antibody from Amersham-Pharmacia. Mammalian Rho proteins were detected using polyclonal antibodies sc-179 (RhoA), sc-87 (Cdc42) and sc-217 (Rac1) from Santa Cruz Biotechnology (San Diego, CA). DNA and RNA isolation, transfer onto nylon membranes and hybridization with ^{32}P-labeled probes were performed as described previously (Rivero *et al*., 1999).

Conventional and fluorescence microscopy

Cells were fixed either in cold methanol (–20°C) or at room temperature with picric acid/paraformaldehyde (15% vol/vol of a saturated aqueous solution of picric acid/2% paraformaldehyde pH 6.0) followed by 70% ethanol. GDI1 was detected using mAb K8-322-2, protein disulfide isomerase using mAb 221-135-1 (Monnat *et al*., 1997), vacuolin using mAb 221-1-1 (Rauchenberger *et al*., 1997) and the A subunit of the V/H^+-ATPase using mAb 221-35-2 (Jenne *et al*., 1998), followed by incubation with Cy3-labeled anti-mouse IgG. Actin was detected using either TRITC-labeled phalloidin (Sigma) or mAb Act-1 (Simpson *et al*., 1984), followed by incubation with Cy3-labeled anti-mouse IgG. Nuclei were stained with DAPI (Sigma).

For conventional transmission and fluorescence microscopy, an Olympus IX70 inverse microscope equipped with a 40$\times$ LCPlanFl 0.6 and a 10$\times$ UplanFl 0.3 objective was used. Images were captured either with a JAI CV-M10 CCD video camera (Stemmer Imaging GmbH, Puchheim, Germany) or a SensiCam cooled CCD video camera (PCO Computer Optics GmbH, Kelheim, Germany). For the chemotaxis assay, cells starved for 6–8 h were transferred onto a glass coverslip with a plastic ring and were stimulated with a glass capillary micropipette (Eppendorf Femtotip) filled with 0.1 M cAMP (Gerisch and Keller, 1981). Time-lapse image series were captured and stored on a computer hard drive at 30 s intervals. The DIAS software (Soltech, Oakdale, IA) was used to trace individual cells along image series and to calculate cell motility parameters (Soll *et al*., 2001). Confocal images were taken with an inverted Leica TCS-SP laser-scanning microscope with a 63$\times$ PL Fluotar 1.32 oil immersion objective. For excitation, the 488 nm argon-ion laser line and the 568 nm krypton-ion laser line were used. Images were processed using the accompanying software.

Two-hybrid assays

DNA fragments encoding *Dictyostelium* GDI1, GDI2, Rho GTPases (Rivero *et al*., 2001) and RasG, and human Rho GTPases (Illenberger *et al*., 1998) were cloned into the pACT2 (GDIs) or the pAS2-1 (GTPases) vector (Clontech, Palo Alto, CA). For construction of a chimera composed of the N-terminal domain of GDI1 fused to GDI2, the N-terminal domain of GDI1 was amplified by PCR. Subsequently, both fragments were joined by conventional cloning methods in pBluescript (Stratagene, La Jolla, CA) and the chimeric DNA fragment was excised and cloned into the pACT vector. Two-hybrid assays were performed following the protocols of the Matchmaker two-hybrid system from Clontech.

Solubilization of membrane-bound recombinant Rho GTPases with soluble GDI

For the production of *Dictyostelium* GST-tagged Rho GTPases in insect cells, cDNAs were cloned into baculovirus transfer vectors pAcG2T or pAcG3X (Pharmingen, San Diego, CA). Preparation of membranes containing recombinant GTPases from baculovirus-infected insect cells and purification of GST and GST–RhoGDI from *Escherichia coli* have been described previously (Illenberger *et al*., 1998). Membranes of insect cells expressing Rho GTPases (1.0 mg of protein each) were incubated with 40 μM GST, GST–RhoGDI, GST–GDI1, His-tagged GDI1, His-tagged GDI2 or the His-tagged chimeric protein composed of the N-terminus of GDI1 fused to GDI2, as described previously (Illenberger *et al*., 1998).

Cell biology methods

To investigate changes in the distribution of the V/H^+-ATPase under osmotic stress conditions, coverslips with cells were incubated for 1 h either in distilled water or in Sörensen phosphate buffer with 0.4 M sorbitol. To investigate the effects of cytochalasin on actin distribution, coverslips with cells were incubated for 1 h in the presence of 20 μM cytochalasin A (Sigma). Cells were then fixed and stained for actin or the vacuolar ATPase.

Cell size, resistance against osmotic shock, phagocytosis, and fluid-phase endo and exocytosis were measured as described previously (Rivero *et al*., 1999). Chemoattractant-induced F-actin formation in aggregation competent cells was quantitated as described previously (Hall *et al*., 1988). Identical procedure was used to determine the F-actin content in unstimulated cells, with the difference that fluorescence values were normalized to the protein content of the sample.

Miscellaneous methods

Standard molecular biology methods were as described by Sambrook and Russell (2001). All PCR products were verified by sequencing, performed at the service laboratory of the Center for Molecular Medicine, Cologne, using an automated sequencer (ABI 377 PRISM, Perkin Elmer, Norwalk, CO).

Supplementary data

Supplementary data are available at *The EMBO Journal* Online.

Acknowledgements

We are grateful to the *Dictyostelium* cDNA and genome sequencing projects for allowing access to DNA sequence information and to the Genome Sequencing Centre at Jena for providing genomic clones. We thank Markus Maniak for providing antibodies against VatA, PDI and vacuolin, Menno Knetsch for providing RacC-Q64L cDNA, David Knecht for kindly allowing access to unpublished results, Angelika A.Noegel for critical reading of the manuscript and Peter Gierschik for support and encouragement. This work was supported by the Deutsche Forschungsgemeinschaft (RI 1034/2-1 and SFB497) and by the Köln Fortune program.

References

Abo,A., Pick,E., Hall,A., Totty,N., Teahan,C.G. and Segal,A.W. (1991) Activation of the NADPH oxidase involves the small GTP-binding protein $p21^{rac1}$. *Nature*, **353**, 668–670.

Becker,M., Matzner,M. and Gerisch,G. (1999) Drainin required for membrane fusion of the contractile vacuole in *Dictyostelium* is the prototype of a protein family also represented in man. *EMBO J.*, **18**, 3305–3316.

Bush,J., Temesvari,L., Rodriguez-Paris,J., Buczynski,G. and Cardelli,J. (1996) A role for a Rab4-like GTPase in endocytosis and in regulation of contractile vacuole structure and function in *Dictyostelium discoideum*. *Mol. Biol. Cell*, **7**, 1623–1638.

Castellano,F., Montcourrier,P. and Chavrier,P. (2000) Membrane recruitment of Rac1 triggers phagocytosis. *J. Cell Sci.*, **113**, 2955–2961.

Chung,C.Y., Lee,S., Briscoe,C., Ellsworth,C. and Firtel,R.A. (2000) Role of Rac in controlling the actin cytoskeleton and chemotaxis in motile cells. *Proc. Natl Acad. Sci. USA*, **97**, 5225–5230.

Clarke,M. and Heuser,J. (1997) Water and ion transport. In Maeda,Y., Inouye,K. and Takeuchi,I. (eds), *Dictyostelium—A Model System for Cell and Developmental Biology*. Universal Academy Press, Inc., Tokyo, Japan, pp. 75–91.

Degani,S., Balzac,F., Brancaccio,M., Guazzone,S., Retta,S.F., Silengo,L., Eva,A. and Tarone,G. (2002) The integrin cytoplasmic domain-associated protein ICAP-1 binds and regulates Rho family GTPases during cell spreading. *J. Cell Biol.*, **156**, 377–387.

DelPozo,M.A., Kiosses,W.B., Alderson,N.B., Meller,N., Hahn,K.M. and Schwartz,M.A. (2002) Integrins regulate GTP-Rac localized effector interactions through dissociation of Rho-GDI. *Nat. Cell Biol.*, **4**, 232–239.

Dumontier,M., Höcht,P., Mintert,U. and Faix,J. (2000) Rac1 GTPases control filopodia formation, cell motility, endocytosis, cytokinesis and development in *Dictyostelium*. *J. Cell Sci.*, **113**, 2253–2265.

Dutartre,H., Davoust,J., Gorvel,J.-P. and Chavrier,P. (1996) Cytokinesis arrest and redistribution of actin-cytoskeleton regulatory components in cells expressing the RhoGTPase CDC42Hs. *J. Cell Sci.*, **109**, 367–377.

Eitzen,G., Thorngren,N. and Wickner,W. (2001) Rho1p and Cdc42p act after Ypt7p to regulate vacuole docking. *EMBO J.*, **20**, 5650–5656.

Ellis,S. and Mellor,H. (2000) Regulation of endocytic traffic by Rho family GTPases. *Trends Cell Biol.*, **10**, 85–88.

Fukumoto,Y., Kaibuchi,K., Hori,Y., Fujioka,H., Araki,S., Ueda,T., Kikuchi,A. and Takai,Y. (1990) Molecular cloning and characterization of a novel type of regulatory protein (GDI) for the rho proteins, ras p21-like small GTP-binding proteins. *Oncogene*, **5**, 1321–1328.

Gerisch,G. and Keller,H.U. (1981) Chemotactic reorientation of granulocytes stimulated with micropipettes containing fMet-Leu-Phe. *J. Cell Sci.*, **52**, 1–10.

Groysman,M., Shifrin,C., Russek,N. and Katzav,S. (2000) Vav, a GDP/GTP nuclotide exchange factor, interacts with GDIs, proteins that inhibit GDP/GTP dissociation. *FEBS Lett.*, **467**, 75–80.

Hall,A. (1998) Rho GTPases and the actin cytoskeleton. *Science*, **279**, 509–514.

Hall,A.L., Schlein,A. and Condeelis,J. (1988) Relationship of pseudopod extension to chemotactic hormone-induced actin polymerization in amoeboid cells. *J. Cell. Biochem.*, **37**, 285–299.

Harris,E., Yoshida,K., Cardelli,J. and Bush,J. (2001) A Rab11-like GTPase associates with and regulates the structure and function of the contractile vacuole system in *Dictyostelium*. *J. Cell Sci.*, **114**, 3035–3045.

Hart,M.J., Maru,Y., Leonard,D., Witte,O.N., Evans,T. and Cerione,R.A. (1992) A GDP dissociation inhibitor that serves as a GTPase inhibitor of the Ras-like protein CDC42Hs. *Science*, **258**, 812–815.

Hoffman,G.R., Nassar,N. and Cerione,R.A. (2000) Structure of the Rho family GTP-binding protein Cdc42 in complex with the multifunctional regulator RhoGDI. *Cell*, **100**, 345–356.

Hori,Y., Kikuchi,A., Isomura,M., Katayama,M., Miura,Y., Fujioka,H., Kaibuchi,K. and Takai,Y. (1991) Post translational modifications of the C-terminal region of the rho protein are important for its interaction with the membranes and inhibitory GDP/GTP exchange proteins. *Oncogene*, **6**, 515–522.

Illenberger,D., Schwald,F., Pimmer,D., Binder,W., Maier,G., Dietrich,A. and Gierschik,P. (1998) Stimulation of phospholipase $C\text{-}\beta_2$ by the Rho GTPases Cdc42Hs and Rac1. *EMBO J.*, **17**, 6241–6249.

Jenne,N., Rauchenberger,R., Hacker,U., Kast,T. and Maniak,M. (1998) Targeted gene disruption reveals a role for vacuolin B in the late endocytic pathway and exocytosis. *J. Cell Sci.*, **111**, 61–70.

Knetsch,M.L.W., Schäfers,N., Horstmann,H. and Manstein,D.J. (2001) The *Dictyostelium* Bcr/Abr-related protein DRG regulates both Rac- and Rab-dependent pathways. *EMBO J.*, **20**, 1620–1629.

Kozma,R., Ahmed,S., Best,A. and Lim,L. (1995) The Ras-related protein Cdc42Hs and bradykinin promote formation of peripheral actin microspikes and filopodia in Swiss 3T3 fibroblasts. *Mol. Cell. Biol.*, **15**, 1942–1952.

Lamaze,C., Chuang,T.-H., Terlecky,L.J., Bokoch,G.M. and Schmid,S.L. (1996) Regulation of receptor-mediated endocytosis by Rho and Rac. *Nature*, **382**, 177–179.

Larochelle,D.A., Vithalani,K.K. and De Lozanne,A. (1997) Role of the *Dictyostelium* racE in cytokinesis: mutational analysis and localization studies by use of green fluorescent protein. *Mol. Biol. Cell*, **8**, 935–944.

Michaelson,D., Silletti,J., Murphy,G., D'Eustachio,P., Rush,M. and Philips,M.R. (2001) Differential localization of Rho GTPases in live cells: regulation by hypervariable regions and RhoGDI binding. *J. Cell Biol.*, **152**, 111–126.

Mondal,M.S., Wang,Z., Seeds,A.M. and Rando,R.R. (2000) The specific binding of small molecule isoprenoids to rhoGDP dissociation inhibitor (rhoGDI). *Biochemistry*, **39**, 406–412.

Monnat,J., Hacker,U., Geissler,H., Rauchenberger,R., Neuhaus,E.M., Maniak,M. and Soldati,T. (1997) *Dictyostelium discoideum* protein disulfide isomerase, an endoplasmic reticulum resident enzyme lacking a KDEL-type retrieval signal. *FEBS Lett.*, **418**, 357–362.

Noegel,A.A. and Schleicher,M. (2000) The actin cytoskeleton of *Dictyostelium*: a story told by mutants. *J. Cell Sci.*, **113**, 759–766.

Olofsson,B. (1999) Rho guanine dissociation inhibitors: pivotal molecules in cellular signalling. *Cell Signal.*, **11**, 545–554.

Palmieri,S.J. *et al.* (2000) Mutant Rac1b expression in *Dictyostelium*: effects on morphology, growth, endocytosis, development and the actin cytoskeleton. *Cell Motil. Cytoskeleton*, **46**, 285–304.

Platko,J.V., Leonard,D.A., Adra,C.N., Shaw,R.J., Cerione,R.A. and Lim,B. (1995) A single residue can modify target-binding affinity and activity of the functional domain of the Rho-subfamily GDP dissociation inhibitors. *Proc. Natl Acad. Sci. USA*, **92**, 2974–2978.

Rauchenberger,R., Hacker,U., Murphy,J., Niewöhner,J. and Maniak,M. (1997) Coronin and vacuolin identify consecutive stages of a late, actin-coated endocytic compartment in *Dictyostelium*. *Curr. Biol.*, **7**, 215–218.

Ridley,A.J. (2001) Rho GTPases and cell migration. *J. Cell Sci.*, **114**, 2713–2722.

Rivero,F., Albrecht,R., Dislich,H., Bracco,E., Graciotti,L., Bozzaro,S. and Noegel,A.A. (1999) RacF1, a novel member of the Rho protein family in *Dictyostelium discoideum*, associates transiently with cell contact areas, macropinosomes and phagosomes. *Mol. Biol. Cell*, **10**, 1205–1219.

Rivero,F., Dislich,H., Glöckner,G. and Noegel,A.A. (2001) The *Dictyostelium* family of Rho-related proteins. *Nucleic Acids Res.*, **29**, 1068–1079.

Sambrook,J. and Russell,D.W. (2001) *Molecular Cloning: A Laboratory Manual*. 3rd edn, Cold Spring Harbor Laboratory Press, Cold Spring Harbor, NY.

Scheffzek,K., Stephan,I., Jensen,O.N., Illenberger,D. and Gierschik,P. (2000) The Rac-RhoGDI complex and the structural basis for the regulation of Rho proteins by RhoGDI. *Nat. Struct. Biol.*, **7**, 122–126.

Seastone,D.J., Lee,E., Bush,J., Knecht,D. and Cardelli,J. (1998) Overexpression of a novel Rho family GTPase, RacC, induces unusual actin-based structures and positively affects phagocytosis in *Dictyostelium discoideum*. *Mol. Biol. Cell*, **9**, 2891–2904.

Simpson,P.A., Spudich,J.A. and Parham,P. (1984) Monoclonal

antibodies prepared against *Dictyostelium* actin: characterization and interaction with actin. *J. Cell Biol.*, **99**, 287–295.

Soll,D.R., Wessels,D., Vos,E. and Johnson,O. (2001) Computer-assisted systems for the analysis of amoeboid cell motility. *Methods Mol. Biol.*, **161**, 45–58.

Takahashi,K., Sasaki,T., Mammoto,A., Takaishi,K., Kameyama,T., Tsukita,S., Tsukita,S. and Takai,Y. (1997) Direct interaction of the Rho GDP dissociation inhibitor with ezrin/radixin/moesin initiates the activation of the Rho small G protein. *J. Biol. Chem.*, **272**, 23371–23375.

Togawa,A. *et al*. (1999) Progressive impairment of kidneys and reproductive organs in mice lacking RhoGDIα. *Oncogene*, **18**, 5373–5380.

Tolias,K.F., Couvillon,A.D., Cantley,L.C. and Carpenter,C.L. (1998) Characterization of Rac1- and RhoGDI-associated lipid kinase signalling complex. *Mol. Cell. Biol.*, **18**, 762–770.

Van Aelst,L. and D'Souza-Schorey,C. (1997) Rho GTPases and signaling networks. *Genes Dev.*, **11**, 2295–2322.

Westphal,M., Jungbluth,A., Heidecker,M., Mühlbauer,B., Heizer,C., Schwarz,J.-M., Marriot,G. and Gerisch,G. (1997) Microfilament dynamics during cell movement and chemotaxis monitored using a GFP-actin fusion. *Curr. Biol.*, **7**, 176–183.

Yin,L., Schwartzberg,P., Scharton-Kersten,T.M., Staudt,L. and Lenardo,M. (1997) Immune responses in mice deficient in Ly-GDI, a lymphoid-specific regulator of Rho GTPases. *Mol. Immunol.*, **34**, 481–491.

Received December 3, 2001; revised May 28, 2002; accepted July 9, 2002